JB Accepts, published online ahead of print on 25 August 2014
J. Bacteriol. doi:10.1128/JB.02095-14

Cell division resets polarity and motility for the bacterium *Myxococcus xanthus*

Running title: *Myxococcus xanthus* cell division resets polarity

Cameron W. Harvey[1,2], Chinedu S. Madukoma[3], Shant Mahserejian[1], Mark S. Alber[1,2,4*], Joshua D. Shrout[3,5*]

[1]Department of Applied and Computational Mathematics and Statistics, University of Notre Dame, Notre Dame, IN, 46556; USA

[2]Department of Physics, University of Notre Dame, Notre Dame, IN, 46556; USA

[3]Department of Civil and Environmental Engineering and Earth Sciences, University of Notre Dame, Notre Dame, IN, 46556; USA

[4]Department of Medicine, Indiana University School of Medicine, Indianapolis, IN, 46202; USA

[5]Department of Biological Sciences, University of Notre Dame, Notre Dame, IN, 46556; USA

[*]for correspondence: joshua.shrout@nd.edu

BYLINE:

Cell division cues *Myxococcus xanthus* progeny to move in opposing directions, which involves asymmetric distribution of the G-protein RomR.

ABSTRACT

Links between cell division and other cellular processes are poorly understood. It is difficult to simultaneously examine division and function for most cell types. Most research probing aspects of cell division has experimented with stationary or immobilized cells, or distinctly asymmetrical cells. Here we take an alternative approach by examining cell division events within motile groups of cells growing on solid media using time-lapse microscopy. A total of 558 cell divisions were identified amongst approximately 12,000 cells. We find an interconnection of division, motility, and polarity for the bacterium *Myxococcus xanthus*. For every division event, motile cells stop moving to divide. Progeny of binary fission subsequently move in opposing directions. This behavior involves *M. xanthus* Frz proteins that regulate *M. xanthus* motility reversals but is independent of type IV pili "S-motility". The inheritance of opposing polarity is correlated with the distribution of the G-protein RomR within these dividing cells. The constriction at the point of division limits the intracellular distribution of RomR. Thus, asymmetric distribution of RomR at the parent cell poles becomes mirrored in new poles initiated at the site of division.

INTRODUCTION

Many approaches to study cell division utilize traits that readily allow for distinction of two progeny. For example, cells displaying "asymmetrical" division traits allow for clear distinction of numerous characteristics that can then be monitored while deciphering other unknowns. *Caulobacter* bacteria are among the best studied with this distinction (1), but other biological examples include: pre-neuron neuroblast brain cells, budding *Saccharomyces cerevisiae*, germline cells of male *Drosophila*, endospore development by *Bacillus* species, and

47 *Mycobacterium* species subjected to environmental nutrient stress (2, 3). While such explicitly
48 distinct examples may be rare, nearly all types of cells display some asymmetrical properties
49 when functioning properly. There are numerous examples of distinctive asymmetrical and
50 polarized attributes of cells (4). However, one difficulty that remains in characterizing
51 asymmetrical properties in biology is distinguishing the timing and order of those intra- and
52 inter-cellular attributes that are transient in nature. Alternative to studying asymmetric cell-types
53 that can be readily differentiated, other research strategies to probe stages of division often
54 examine stationary or immobilized cells.

55 *M. xanthus* is one of many Myxobacteria, common soil microbes that grow readily in
56 environments rich in complex organics, such as those containing decaying plants (5) or other
57 bacteria (6). *M. xanthus* cells exhibit a symmetric morphology. The specific mechanism and
58 dynamics of *M. xanthus* cell division, like that of most non-model organisms, is not entirely
59 known. *M. xanthus* is among many bacteria lacking a clear MinCD system that drives
60 recruitment of FtsZ for division. It is known that the middle of *M. xanthus* cells is marked by
61 PomZ, which likely recruits FtsZ (7) for proper division.

62 *M. xanthus* has been studied largely as a model organism to understand cellular motility
63 and the development of self-organized swarming groups that aggregate to form sporulating
64 fruiting bodies. Upon starvation, *M. xanthus* glides in a well-choreographed manner to aggregate
65 into clusters containing roughly 10^6 cells, which then develop into *M. xanthus* fruiting bodies (8-
66 13). *M. xanthus* does not move by flagella, but displays two distinct motility phenotypes
67 described as A-motility and S-motility. During A-motility, cells move with or without the
68 company of neighbor cells and do so preferentially in tracks of polysaccharide slime; the specific
69 mechanism(s) of A-motility remain under investigation, and proposed models include propulsion

by slime secretion, focal adhesions, or a helical motor (14-17). During S-motility, *M. xanthus* cells attach to other cells using type IV pili (TFP) at the leading pole to pull the cell forward when the pilus tips have bound to exopolysaccharide covering cells ahead (18-20). Another important facet of *M. xanthus* movement is that this bacterium regularly reverses direction (21); during reversal the leading and lagging poles switch on the order of seconds (21-23). Reversals have been traced to the action of a small G-protein switch (24, 25), and these reversals are induced by the Frz system (26-28). At the core of the Frz system is a two component signal transduction system consisting of FrzCD, a methyl accepting chemo-receptor (MCP) domain, and FrzE, a histidine-kinase protein (29-31). The Frz proteins are homologous to Che proteins that confer swimming chemotaxis in several bacteria (32, 33). However, the Frz signal transducing proteins lack an extracellular receptor to confer classical chemotaxis (26, 29), which is similar to other signal transduction networks, such as Wsp in *P. aeruginosa*, where the input mechanism has not been fully elucidated (34-36). Several proteins associated with motility and reversals of *M. xanthus* have been shown to display localized traits (24, 25, 27, 28, 37-40), however the biochemistry and regulation governing motility behavior of *M. xanthus* continues to be investigated. The ability to reverse has been shown crucial for maximizing the overall spreading of *M. xanthus* populations by minimizing and resolving collisions.

Here we investigate *M. xanthus* cell division under conditions that promote surface motility. We report that cell division and surface motility are coordinated for the bacterium *M. xanthus* as polarity is reset at the time of division. When surface motile, we demonstrate that *M. xanthus* cells always pause their movement to complete binary cell division. Further, these dividing *M. xanthus* cells display asymmetrical properties with respect to inherited polarity. After a consistent period, the two progeny are predisposed to resume movement in opposing

93 directions. These pauses for division dominate over any intercellular interactions as even cells
94 that are part of a motile cluster of cells will dissociate and stop prior to cell division. This pause
95 and polarity behavior involves the Frz reversal proteins FrzCD and FrzE but is independent of
96 type IV pili-mediated *M. xanthus* S-motility. While the timing basis for these division pauses is
97 currently unclear, these dividing cells plainly display asymmetric properties that coincide with
98 cell division. We demonstrate that opposing polarity of new progeny involves an asymmetric
99 distribution of the G-protein RomR as parent cell polar distributions of RomR become mirrored
100 in new poles initiated at the site of division.
101
102 **MATERIALS AND METHODS**
103 ***Bacterial strains and growth medium.*** All strains of *Myxococcus xanthus* utilized for this
104 study are included in Table 1. Strains were maintained by growing on CTT agar plates (41).
105 ***Image chamber assembly and inoculation.*** Imaging chambers were adapted from the
106 imaging plate complex described by Taylor and Welch (42). Briefly, we constructed a modified
107 imaging chamber using 20 mm-diameter and 2.0 mm-thick Grace Bio-Labs (Bend, Oregon)
108 silicon gaskets. Sterile, melted CTT agar (2%) was pipetted into the gasket fixed to a microscope
109 slide. A second microscope slide was place on top of gasket sandwiching agar and gasket
110 between two slides. The assembly was held together by black metal binder clips and stored at
111 4°C to cure.
112 For inoculation, a chamber was moved from 4°C storage and warmed to room
113 temperature before removing the top coverslip. Chambers were inoculated with *M. xanthus* using
114 a sterile platinum wire. The uncovered chamber was placed in an empty petri dish and sealed
115 with parafilm to limit agar dying. Immediately prior to imaging, a cover slip was placed on the

chamber and pressed firmly around the perimeter to seal the thin agar disc (a thin liquid layer formed between the cover slip and agar disc).

Cell Division Measurements. Tracking of cell division was done manually by screening individual frames of time-lapse movies of *M. xanthus*, which typically included 50-100 cells near the swarm edge in the imaging chambers used. The position, direction and initial stoppage time was noted for each parent cell. Dividing cells for which the complete division sequence could not be chronicled were excluded from further analysis.

The two progeny cells were then designated by the last known movement direction of the parent cell. The leading half of the cell was designated as the "leading" cell, while the trailing half was designated as the "lagging" cell. The cell was observed until both progeny initiated movement and the time and direction (with respect to the parent) of each new cell was recorded. Despite this straight forward approach, interaction of dividing cells with neighboring cells presented the additional challenge of distinguishing between active movement by any cell from passive movement brought about by the movement of surrounding cells. To measure the pause duration of a division, we measured the number of frames between that last observed motion of the parent cell and the resumption of motion by either of the two progeny (the recorded pause duration does not include the extra time needed for the second progeny cell to resume motion).

Polarity Inheritance Measurements. Cell polarity for newly divided cells was compared to the last direction recorded for the pre-division parent cell. Polarity of the parent cell was assigned according to the last observed moving direction. Accordingly, the polarity of the new cells was assigned by their initial movement direction in reference to the parent cell.

We record the motility start time of each newly divided cell independently. While many division events showed initiation of movement by both progeny cells in the same frame of the

time-lapse data, more than half of the data show one progeny initiating movement before the other. To distinguish between synchronous and asynchronous motility, events were identified as either 1) leading cell starting first, 2) lagging cell starting first, or 3) both progeny cells starting together (synchronous). In order to establish a clear priority among the restarts, a threshold of 30 seconds between motility events was chosen before cells were counted as asynchronous.

Dynamic distribution analysis of RomR. RomR-Gfp was tracked over the length of dividing cells for strain JS1. Each pre-division sequence was manually delineated from the rest of the image for all frames. This segmented sequence was then processed using a custom Matlab program to assign the delineated cell in each frame to a line representing the central longitudinal axis of the cell. Separately in ImageJ, the green fluorescent channel was processed using the "despeckle" function followed by filtering with a Gaussian blur to smooth the image. The linear distribution of RomR was obtained by averaging fluorescence intensity of RomR-GFP over numerous 3×3 pixel blocks centered on each pixel of the central axis line for a cell. This cell central axis line was then sectioned into 60 equally spaced points where 0 corresponded to the head (leading pole) of the cell and 1 corresponded to the tail (lagging pole). After a clear separation of cell progeny, the original 60 points were split into 30 points for each progeny, where 0 to 0.5 corresponded to the leading cell and 0.5 to 1 corresponded to the lagging cell. RomR-GFP intensity was spatially quantified as the fluorescent intensity at each of the 60 points along the 0-1.0 relative cell length. The dynamic intensity was obtained for all frames of a time-lapse movie and plotted using the surface plot in Matlab.

RomR distribution was also analyzed to consider relative abundance of RomR over a sequence of a dividing cell and its two progeny. We considered the two (old) poles of the parent cell and the cell midpoint from which two new poles will form, the dividing cell midpoint, and

the subsequent two new poles. Localized RomR levels were measured within 10×10 pixel areas centered at each of these three localization foci. Mean Gfp intensity was measured for the box for each frame of the image sequence. For these larger pixel area measurements, a background subtraction was applied to each measurement by selecting a 10×10 pixel region away from the cell. Relative abundance was normalized by dividing each measurement (3 compartments, 48 frames) by the mean RomR-Gfp intensity measured in frame 1 of the lagging pole compartment for the pre-division images. For the post-division sequence, we normalize by dividing each measurement (2 compartments, 30 frames) by the mean RomR-Gfp intensity in frame 6 of the lagging cell's new pole compartment (i.e., the first frame where the two poles are distinguishable).

The ratio of intensity of the leading and lagging pole was averaged over multiple frames prior to the point of separation. Contact with neighboring cells (and thus RomR signal coming from other cells) interfered with measurements during the division pause limiting the number of frames available for certain division sequences. Following division, the first 4 frames in which the two new poles could be distinguished were used to get an average value of the ratio between the leading cell's new pole and the lagging cell's new pole.

Growth Rate. Surface growth rates for each strain were obtained by quantifying fluorescence over time using a fluorescent imaging method (43). Briefly, *M. xanthus* colonies were grown on one 150 mm CTT agar (1.5%) plate containing 8 µL per 100 mL of Syto64 bacterial-staining dye (Life Technologies, Grand Island, NY). Fluorescent images of swarm plates were acquired using a Carestream Multispectral FX (MSFX) imaging station (Carestream Health, Woodbridge, CT) using excitation and emission wavelengths of 590/670nm, respectively. Time lapse images of the whole plate were recorded every ten minutes. Growth

185 rates for each strain were determined by calculating the mean of fluorescent intensity of three
186 replicates for each strain.

187 ***Velocity Measurements.*** For each strain, 15-20 cells were tracked manually using the
188 ImageJ plugin MtrackJ from a representative time-lapse data set. The leading edge of a tracked
189 cell was identified in approximately 40 successive frames to calculate an average velocities for
190 each tracked cell. The average velocity of the strain was then determined by averaging the
191 velocities of all tracked cells. Because of the hyper-reversing attributes of Δ*frzCD* strain
192 DW706, only 10-15 frames could typically be tracked before the cell reversed direction—for this
193 strain, a lower number of frames (10-15) were tracked for more cells (30 cells) were used to
194 calculate the average cell velocity. These measured velocities were representative of the cell
195 speeds for these strains when grown and imaged in our chambers described above. Certainly
196 some differences for cell speed can be expected from previous reports in the literature given the
197 different environmental conditions of our chamber experiments. However, all cell speed data
198 presented here provides the relative speed for strains examined for this work conducted under the
199 same conditions as the division measurements.

200 ***Expansion Measurements.*** The expansion rate or swarming rate for each strain was
201 obtained by a similar protocol as that used in (44). A fresh agar plate was stab inoculated with a
202 platinum wire containing growing *M. xanthus* cells. Over the course of 1-2 weeks, the diameter
203 of the expanding colonies was measured with a ruler.

204 ***Statistical Analysis.*** Pause duration for the *M. xanthus* strains were analyzed with
205 ANOVA1 to determine that the different data sets do not have the same distribution. To
206 determine which strains were significantly different from each other, a mean comparison
207 (multicompare function in Matlab which used results from ANOVA1) was used to determine

whether or not the 95% confidence interval for the means of any two strains overlapped. Non-overlapping intervals were recognized as significantly differing.

RESULTS

M. xanthus cells pause to divide. While imaging *M. xanthus* growing under nutrient-rich, motility-favorable conditions using time-lapse microscopy, we observe that motile cells stop as a precursor step to binary cell division. Figure 1 shows a representative example where a motile *M. xanthus* cell pauses and remains paused until this cell has completed binary cell division (a movie of the entire time-lapse series is included as Supplemental Movie S1). We subsequently probe for cell division events of *M. xanthus* by systematically analyzing movement of approximately 12,000 cells. While similar stoppage of predivision cells has been observed previously by Reichenbach, et al. (45), our analysis shows this not being an occasional or random event. Every dividing cell (n = 558) in our experiments pauses prior to this division—no cells were observed to divide while motile. On average for two common *M. xanthus* wildtype strains DK1622 and DZ2, these motility pauses are approximately 19 minutes in duration before the two daughter cells resume movement (Table 2). Further, only predivision cells pause for these extended durations. Motile, non-dividing cells that stop (either to reverse or continue in the same direction) all exhibit a pause duration of less than one minute, which is in the range of reversal pauses that have been specifically measured previously (46, 47).

The requirement and duration of these pauses are notably unaffected by physical interactions with other *M. xanthus* cells. Predivision cells that are moving over surfaces in clusters dissociate from clusters and stop. Yet this stoppage is not a rigid, immovable fixation of cells to the surface as stopped cells can be "jostled" or partially displaced. In general, however,

predivision cells are notably unaffected by physical interactions with other *M. xanthus* cells. Dividing cells located within either low- or moderate-density populations show the same behavior as isolated cells. Key stages showing active motility, pausing of motility, interaction of paused cells with other motile cells, cell division, and resumption of motility after division for four different parent cells in the same field of view are included as Figure 2 (with the entire sequence included as Movie S2). We find that group interactions are secondary to unicellular behavior associated with *M. xanthus* cell division—pausing for cell division was dominant over any intercellular interaction. Additionally, no distinction in the pause behavior was found between dividing cells that were in contact with other cells and the dividing cells that were isolated. While pre-division cells that stop do not remain absolutely fixed to the surface, these cells do not join in clusters of motile cells upon cell-cell contact as their neighbors (Movie S2). Clearly these predivision cells are able to dissociate from both exopolysaccharide-, cell wall-, and pili-dependent associations of not just their own, but also other cells, to facilitate these pauses. For all dividing cells we tracked in our experiments, the behavior and regulation of cell division is dominant over numerous motility and cell-cell phenotypes that have been documented under similar growth conditions.

Predivision pauses involve Frz but are independent of S-motility. We track motility and divisions of select motility mutants to probe for factors that are important to regulation of these predivision pauses. Because these strains are known to display differing motility and growth characteristics, we measure both motility and growth attributes of these strains for the growth conditions used in these experiments (Table 2). Of the mutations examined, only Δ*frzE* and Δ*frzCD* strains show a significant deviation in stoppage from wildtype cells—the pre-division pauses for Δ*frzE* and Δ*frzCD* strains were 26.5± 0.9 min and 22.3± 1.0 min, respectively (Figure

254 3). The pre-division pauses of Δ*frzF* and Δ*frzG* strains are are statistically similar to those of the
255 wildtype strains. Similar pausing behavior is also detailed for a Δ*pilA* strain that has no TFP;
256 thus, TFP are not needed for this behavior and likely function only after cell division is complete.
257 Differences in gliding speed, swarm expansion rate, or growth rate did not correlate with
258 the length of the pre-divisional pause. As we describe above, the pause duration for the division
259 events for DK1622 wildtype, DZ2 wildtype, and DK8621 Δ*pilA* S-motility mutant are essentially
260 the same (~19 minutes). Because these strains are known to display differing motility and growth
261 characteristics, we measured both motility and growth attributes of these strains for the growth
262 conditions used in these experiments (Table 2). No attribute or pattern emerges that correlates
263 with the pause duration for division and we are unable to explain the notable variation in pause
264 period for these pre-division cells (Figure 3). The surface growth rate of DK1622 (and DK1622
265 mutants) is marginally slower than DZ2 for the growth conditions used here, which is
266 comparable with other studies (48-51). The minimum doubling times for DK1622 and DZ2 are
267 4.8 ±0.6 hours and 3.6 ±0.1 hours, respectively.
268 ***Dividing cells inherit polarity.*** After binary cell division is complete and progeny
269 separate, we demonstrate that *M. xanthus* progeny are programmed to move in opposite
270 directions. Newly divided cells were categorized according to their direction of movement. For
271 both wildtype and Δ*pilA* strains, the leading cell (in reference to orientation of the predivision
272 cell) moves in the same direction as the parent cell and the lagging cell moves in the opposite
273 direction for approximately 90% of recorded events (Figure 4). For nearly all of the remaining
274 events (~10% of total), the two progeny initiate movement in the same direction (Movie S3) with
275 no obvious bias towards the leading or lagging cell direction. For just one out of 288 division
276 events tracked for these strains, a “crossing” phenotype is observed where the leading and

277 lagging cells crossed each other. No distinct bias is apparent for the timing of movement after
278 division as progeny pairs resume movement with either cell starting first or progeny initiating
279 movement at the same time (Figure S1). Two of the four Frz-system reversal mutants also show
280 markedly less asymmetry of motility polarity; these *frzCD* and *frzE* mutant progeny are as likely
281 to have initiate movement in the direction of the parent (leading) cell as to move in opposite
282 directions (Figure 4). The *frzG* and *frzF* mutant progeny exhibit the same initial movement
283 patterns as wildtype.

284 ***Distribution of RomR is asymmetric in new poles at division.*** Our analysis detects no
285 unique cell behavioral traits (such as a change in velocity) for predivision or newly divided cells
286 in comparison to other *M. xanthus* cells. However, we find that intracellular localization of
287 motility proteins is cued with the pausing of predivision cells. We investigate dynamics of the
288 protein RomR during cell division; RomR is known to interact with both the Frz system and the
289 G-protein switch of MglA/MglB that mediate *M. xanthus* reversals (27, 28) and is thought to
290 become localized to poles when non-phosphorylated, but released from poles when
291 phosphorylated (52). Inspection of RomR-Gfp fusions show that recruitment of RomR to the
292 middle of predivisional cells begins shortly after a mother cell pauses motility for division
293 (Figure 5). (A movie of the entire time-lapse series is included as Supplemental Movie S4.) This
294 recruitment of RomR to the site of division occurs while the distribution of RomR at the poles of
295 the parent cell (showing higher levels of RomR present at the lagging pole) is nearly static. Most
296 remarkably, the recruitment of RomR at the site of division shows a striking asymmetry between
297 the two progeny. The level of asymmetry in RomR distribution at the old poles of the parent cell
298 becomes mirrored in the new poles at the site of division, which we have measured using RomR-
299 GFP (Figure S2). While the actual ratio of RomR measured at the poles varies (between 0.43 to

0.83 ratio of RomR leading/lagging pole), the mirroring of these levels in new progeny is very consistent (1.06 ±0.2 ratio of new poles inheriting old pole RomR in both progeny). The RomR-Gfp level at the cell midpoint increases from 20% to 40% (relative to the lagging pole) during the pause. As the progeny begin to pull apart, the new lagging cell (that initiates movement in the opposite direction) exhibits much higher levels of RomR at the newly formed cell pole as compared to the new pole of the leading cell. Thus, RomR is preferentially directed to a specific side at the site of division while the relative abundance of RomR at the previous cell poles is essentially unchanged. Furthermore, the new pole of the leading cell is approximately 45% of the RomR-Gfp level of the new pole of the lagging cell for the first minute after separation. The RomR-Gfp of this lagging cell new pole then abruptly doubles. Such front-abundant distributions of RomR within motile cells are counter-intuitive to our current understanding of the role for RomR in establishing polarity of motility for *M. xanthus* (27, 53). Previously, it would have been predicted that RomR should be most abundant at the rear pole of motile cells. Here we note that the newly divided lagging cell initiates opposing motility despite having lower levels of RomR at the newly formed lagging pole in comparison to the leading pole (i.e., the previously lagging pole of the parent cell). Also, the leading cell that retains the same polarity as the parent cell is able to resume motility in this direction despite a lack of RomR abundance at the cell rear. Thus, RomR appears needed to establish motility in a new direction but not to resume an existing polarity. After 3-5 minutes of motion post-division, the lagging poles in each of these progeny establish RomR levels greater than or equal to their leading poles.

The necessity of proper RomR accumulation at the poles to set opposing polarity in new progeny is confirmed by monitoring RomR-Gfp in a *frzCD* mutant strain. In a *frzCD* background, *M. xanthus* progeny do not necessarily move in opposing directions (Figure 4) and

323 the Frz system that guides RomR accumulation is disrupted (27, 28). We find the localization of
324 RomR in a *frzCD* mutant is altered throughout the cell cycle as RomR clusters are observed at
325 multiple locations within all cells in a field of view (Figure 6). In addition to RomR-Gfp
326 localized to poles at various ratios, a total of 3-4 RomR accumulation sites are observed. Thus a
327 proper polarity of RomR is never established and progeny have a more random polarity after
328 division (Movie S5). Over time, the highest intensity RomR-Gfp does not appreciably oscillate
329 in this *frzCD* strain as in wildtype, suggesting that disassembly of RomR puncta is distorted in
330 this *frzCD* background.
331
332 **DISCUSSION**
333 Using high-resolution time-lapse microscopy to image *M. xanthus* motility of
334 approximately 12,000 cells, we find that all dividing cells pause prior to division. We confirm
335 this behavior for the most commonly studied *M. xanthus* wildtype backgrounds DK1622 and
336 DZ2. Our analysis detected no unique traits for predivision cells prior to their pause or for new
337 motile progeny in comparison to the other *M. xanthus* cells. We further demonstrate that after
338 division, progeny move in opposing directions. This pausing and polarity behavior involves the
339 Frz cascade as *frzCD* and *frzE* mutations disrupted these patterns. We conclude this behavior
340 involves *M. xanthus* A-motility as a *pilA* deficient S-motility mutant exhibited the same behavior
341 as wildtype.
342 The requirement and duration of these pauses were notably unaffected by physical
343 interactions with other *M. xanthus* cells. This suggests a layer of complexity for associations of
344 *M. xanthus* and other organisms that has not been considered previously—promotion of
345 intercellular activity by neighboring cells can be both blocked and undone by predivision cells.
346 Several studies have shown the importance of different biochemical and physical components

that promote cell-cell interaction (11, 18, 21, 22, 44, 54-56), group alignment (21, 44, 56), and group motility (19, 20, 44, 57, 58) of *M. xanthus*. However, our results show that pausing for cell division dominates over any tested intercellular interactions with distinction of pause behavior with dividing cells that were in contact with other cells as compared to dividing cells that were isolated. Clearly predivision cells are able to dissociate from both polysaccharide-, cell wall-, and pili-dependent associations of not just their own, but also other cells, to facilitate these pauses. This suggests a layer of complexity for such associations that has not been considered previously—we find the behavior and regulation of cell division is dominant over numerous motility and cell-cell phenotypes such that promotion of intercellular activity by neighboring cells can be both blocked and undone by predivision cells. While these predivision pauses were independent of S-motility, any pili-mediated effects actually appear to be negated as *M. xanthus* pauses for division.

While most *M. xanthus* progeny displayed these asymmetric polarity traits, the timing of their movement showed no clear pattern. After division, the predominant phenotype observed was for both cells to initiate movement at essentially the same time. The novelty of this synchronous or un-favored timing is not yet clear as few studies have examined the onset of motility for newly divided cells. Certainly *Caulobacter crescentus* shows highly asynchronous behavior as one attached cell yields one motile cell during division (1). Somewhat similarly, the TFP-motile bacterium, *Pseudomonas aeruginosa*, has exhibited that one divided cell remains attached for surface-attached division events while the other may be motile (59).

The specific mechanism and dynamics of *M. xanthus* cell division, like that of most non-model organisms, is not entirely known. *M. xanthus* is among many bacteria lacking a clear MinCD system that drives recruitment of FtsZ for division. It is known that the middle of *M.*

370 *xanthus* cells is marked by the ParA-like protein PomZ (7). There is support for an association of
371 PomZ with setting *M. xanthus* motility as *pomZ* (originally annotated as *agmE*) was originally
372 identified as a partial A-motility mutant.
373 We describe the resetting of polarity for *M. xanthus* at division by correlating
374 accumulation of RomR at newly formed cell poles with cell division (Figure 7). Our results are
375 consistent with an explanation that pausing of motility is a well-ordered step of the cell cycle.
376 Recent evidence of the detailed orchestration of ParA/ParB important to chromosomal
377 segregation suggest a distinct cycle of approximately four hours where the division into two cells
378 accounts for 30-60 minutes (60, 61). Based on our results, we link cell division with establishing
379 opposing motility polarity of progeny by considering possible distribution scenarios of RomR.
380 We assume that sufficient phosphorylated-RomR is diffusing freely throughout the cell (Figure
381 7). As motility is paused for these predivision cells, we deduce from our experiments that RomR
382 has not yet begun to accumulate via dephosphorylation at the site of division (Figure 5), but
383 continues to diffuse freely in the phosphorylated state. However, we offer that diffusion across
384 the entire predivisional cell starts to become limited at this stage (Figure 7C) due to the
385 constriction of cell division limiting flow between the two cell ends. This constriction also
386 introduces a morphology change as curvature at the predivisional cell middle is initiated—we
387 propose RomR recognizes some component of this developing cell pole as it must recognize
388 existing poles. This may be directly associated with *M. xanthus* ParA, which is known to localize
389 to cell poles and sites of division (60, 61). While diffusion of RomR continues, the level of
390 asymmetry in RomR distribution at the old poles of the parent cell becomes mirrored in the new
391 poles at the site of division, which we have measured using RomR-GFP (Figure S2). While the
392 actual ratio of RomR measured at the poles varies for any single cell (between 0.43 to 0.83 ratio

of RomR leading/lagging pole), the mirroring of these levels from parent to progeny is very consistent (1.06 ±0.2 ratio of new poles inheriting old pole RomR in both progeny). Upon completion of cell division, the accumulation of RomR in the lagging cell is sufficient to recruit MglB to initiate a new direction explaining why we see progeny move away from each other following division.

Morphologically symmetrical *M. xanthus* cells inherit a clear asymmetry in the distribution of proteins that confer their motility. We propose this asymmetry is mirrored at the parent cell midpoint due to the process of division to explain the opposing polarity we observe when division is complete. This proposed mechanism would be sensitive at the time of motility pausing to the distribution of RomR, which is known to switch from the asymmetric pattern to a short-lived symmetric pattern to the opposite asymmetric pattern during cell directional reversals (52). Thus disruption to the Frz system, which effects reversal timing, would be expected to disrupt the polarity pattern inherited by daughter cells as seen in our experiments. Because most cell types are symmetrical, like the *M. xanthus* cells we examined here, gaining more insight into the coordination cascade that regulates this phenotype may useful to understand other processes that are associated with cell division.

ACKNOWLEDGEMENTS

This work was funded by a National Institute of Health grant (R01GM100470).

Strains and helpful discussion were provided by John Kirby (DZ2, DZ4482, and DZ4483), University of Iowa; Lotte Søgaard-Andersen (pSH1208), Max Planck Institute for

Terrestrial Microbiology; and Dan Wall (DK1240, DK7881, DK8621, and DW706), University of Wyoming.

Assistance with some measurements was provided by Eric Fein and Daniel Alber.

REFERENCES

1. **Hughes V, Jiang C, Brun Y.** 2012. *Caulobacter crescentus*. Curr. Biol. **22:**R507-R509.
2. **Kirsebom LA, Dasgupta S, Fredrik Pettersson BM.** 2012. Pleiomorphism in *Mycobacterium*, p. 81-112. *In* Sima S, Geoffrey MG (ed.), Advances in Applied Microbiology, vol. 80. Academic Press.
3. **Horvitz HR, Herskowitz I.** 1992. Mechanisms of asymmetric cell division: Two Bs or not two Bs, that is the question. Cell **68:**237-255.
4. **Brown PJB, Kysela DT, Brun YV.** 2011. Polarity and the diversity of growth mechanisms in bacteria. Semin. Cell Dev. Biol. **22:**790-798.
5. **Reichenbach H.** 1999. The ecology of the myxobacteria. Environ. Microbiol. **1:**15-21.
6. **Berleman JE, Scott J, Chumley T, Kirby JR.** 2008. Predataxis behavior in *Myxococcus xanthus*. Proc. Natl. Acad. Sci. USA **105:**17127-17132.
7. **Treuner-Lange A, Aguiluz K, van der Does C, Gómez-Santos N, Harms A, Schumacher D, Lenz P, Hoppert M, Kahnt J, Muñoz-Dorado J, Søgaard-Andersen L.** 2013. PomZ, a ParA-like protein, regulates Z-ring formation and cell division in *Myxococcus xanthus*. Mol. Microbiol. **87:**235-253.
8. **Campos JM, Zusman DR.** 1975. Regulation of development in *Myxococcus xanthus*: effect of 3':5'-cyclic AMP, ADP, and nutrition. Proc. Natl. Acad. Sci. USA **72:**518-522.
9. **Xie C, Zhang H, Shimkets LJ, Igoshin OA.** 2011. Statistical image analysis reveals features affecting fates of *Myxococcus xanthus* developmental aggregates. Proc. Natl. Acad. Sci. USA **108:**5915-5920.
10. **Zhang H, Angus S, Tran M, Xie C, Igoshin OA, Welch RD.** 2011. Quantifying aggregation dynamics during *Myxococcus xanthus* development. J. Bacteriol. **193:**5164-5170.
11. **Dana JR, Shimkets LJ.** 1993. Regulation of cohesion-dependent cell interactions in *Myxococcus xanthus*. J. Bacteriol. **175:**3636-3647.
12. **Sozinova O, Jiang Y, Kaiser D, Alber M.** 2006. A three-dimensional model of *Myxobacterial* fruiting-body formation. Proc. Natl. Acad. Sci. USA **103:**17255-17259.
13. **Harvey CW, Du H, Xu Z, Kaiser D, Aranson I, Alber M.** 2012. Interconnected Cavernous Structure of Bacterial Fruiting Bodies. PLoS Comput. Biol. **8:**e1002850.
14. **Koch MK, Hoiczyk E.** 2013. Characterization of myxobacterial A-motility: insights from microcinematographic observations. J. Basic Microbiol.
15. **Kaiser D, Robinson M, Kroos L.** 2010. Myxobacteria, polarity, and multicellular morphogenesis. Cold Spring Harbor Perspectives in Biology **2:**a000380.
16. **Balagam R, Litwin DB, Czerwinski F, Sun M, Kaplan HB, Shaevitz JW, Igoshin OA.** 2014. *Myxococcus xanthus* gliding motors are elastically coupled to the substrate as

predicted by the focal adhesion model of gliding motility. PLoS Comput. Biol. **10:**e1003619.

17. **Nan B, Zusman DR.** 2011. Uncovering the Mystery of Gliding Motility in the Myxobacteria. Annu. Rev. Genet. **45:**21-39.
18. **Kaiser D.** 1979. Social gliding is correlated with the presence of pili in *Myxococcus xanthus*. Proc. Natl. Acad. Sci. USA **76:**5952-5956.
19. **Youderian P, Hartzell PL.** 2007. Triple mutants uncover three new genes required for social motility in *Myxococcus xanthus*. Genetics **177:**557-566.
20. **Lu A, Cho K, Black WP, Duan X-y, Lux R, Yang Z, Kaplan HB, Zusman DR, Shi W.** 2005. Exopolysaccharide biosynthesis genes required for social motility in *Myxococcus xanthus*. Mol. Microbiol. **55:**206-220.
21. **Wu YL, Kaiser AD, Jiang Y, Alber MS.** 2009. Periodic reversal of direction allows *Myxobacteria* to swarm. Proc. Natl. Acad. Sci. USA **106:**1222-1227.
22. **Mauriello EM, Astling DP, Sliusarenko O, Zusman DR.** 2009. Localization of a bacterial cytoplasmic receptor is dynamic and changes with cell-cell contacts. Proc. Natl. Acad. Sci. USA **106:**4852-4857.
23. **Yu R, Kaiser D.** 2007. Gliding motility and polarized slime secretion. Mol. Microbiol. **63:**454-467.
24. **Leonardy S, Miertzschke M, Bulyha I, Sperling E, Wittinghofer A, Søgaard-Andersen L.** 2010. Regulation of dynamic polarity switching in bacteria by a Ras-like G-protein and its cognate GAP. EMBO J. **29:**2276-2289.
25. **Zhang Y, Franco M, Ducret A, Mignot T.** 2010. A bacterial Ras-like small GTP-binding protein and its cognate GAP establish a dynamic spatial polarity axis to control directed motility. PLoS Biol. **8:**e1000430.
26. **Blackhart BD, Zusman DR.** 1985. "Frizzy" genes of *Myxococcus xanthus* are involved in control of frequency of reversal of gliding motility. Proc. Natl. Acad. Sci. USA **82:**8767-8770.
27. **Keilberg D, Wuichet K, Drescher F, Søgaard-Andersen L.** 2012. A response regulator interfaces between the Frz chemosensory system and the MglA/MglB GTPase/GAP module to regulate polarity in *Myxococcus xanthus*. PLoS Genet. **8:**e1002951.
28. **Zhang Y, Guzzo M, Ducret A, Li Y-Z, Mignot T.** 2012. A Dynamic Response Regulator Protein Modulates G-Protein–Dependent Polarity in the Bacterium *Myxococcus xanthus*. PLoS Genet. **8:**e1002872.
29. **Bustamante VH, Martinez-Flores I, Vlamakis HC, Zusman DR.** 2004. Analysis of the Frz signal transduction system of *Myxococcus xanthus* shows the importance of the conserved C-terminal region of the cytoplasmic chemoreceptor FrzCD in sensing signals. Mol. Microbiol. **53:**1501-1513.
30. **Inclán YF, Laurent S, Zusman DR.** 2008. The receiver domain of FrzE, a CheA–CheY fusion protein, regulates the CheA histidine kinase activity and downstream signalling to the A- and S-motility systems of *Myxococcus xanthus*. Mol. Microbiol. **68:**1328-1339.
31. **Scott AE, Simon E, Park SK, Andrews P, Zusman DR.** 2008. Site-specific receptor methylation of FrzCD in *Myxococcus xanthus* is controlled by a tetra-trico peptide repeat (TPR) containing regulatory domain of the FrzF methyltransferase. Mol. Microbiol. **69:**724-735.
32. **Wadhams GH, Armitage JP.** 2004. Making sense of it all: Bacterial chemotaxis. Nat. Rev. Mol. Cell Biol. **5:**1024-1037.

33. **Wolfe AJ, Conley MP, Kramer TJ, Berg HC.** 1987. Reconstitution of signaling in bacterial chemotaxis. J. Bacteriol. **169:**1878-1885.
34. **Hickman JW, Tifrea DF, Harwood CS.** 2005. A chemosensory system that regulates biofilm formation through modulation of cyclic diguanylate levels. Proc. Natl. Acad. Sci. USA **102:**14422-14427.
35. **Huangyutitham V, Guvener ZT, Harwood CS.** 2013. Subcellular clustering of the phosphorylated WspR response regulator protein stimulates its diguanylate cyclase activity. mBio **4:**e00242-00213.
36. **O'Connor JR, Kuwada NJ, Huangyutitham V, Wiggins PA, Harwood CS.** 2012. Surface sensing and lateral subcellular localization of WspA, the receptor in a chemosensory-like system leading to c-di-GMP production. Mol. Microbiol. **86:**720-729.
37. **Bulyha I, Lindow S, Lin L, Bolte K, Wuichet K, Kahnt J, van der Does C, Thanbichler M, Søgaard-Andersen L.** 2013. Two small GTPases act in concert with the bactofilin cytoskeleton to regulate dynamic bacterial cell polarity. Dev. Cell **25:**119-131.
38. **Kaimer C, Zusman DR.** 2013. Phosphorylation-dependent localization of the response regulator FrzZ signals cell reversals in *Myxococcus xanthus*. Mol. Microbiol. **88:**740-753.
39. **Nudleman E, Wall D, Kaiser D.** 2006. Polar assembly of the type IV pilus secretin in Myxococcus xanthus. Mol. Microbiol. **60:**16-29.
40. **Bulyha I, Schmidt C, Lenz P, Jakovljevic V, Hone A, Maier B, Hoppert M, Søgaard-Andersen L.** 2009. Regulation of the type IV pili molecular machine by dynamic localization of two motor proteins. Mol. Microbiol. **74:**691-706.
41. **Hodgkin J, Kaiser D.** 1977. Cell-to-cell stimulation of movement in nonmotile mutants of *Myxococcus*. Proc. Natl. Acad. Sci. USA **74:**2938-2942.
42. **Taylor RG, Welch RD.** 2010. Recording multicellular behavior in *Myxococcus xanthus* biofilms using time-lapse microcinematography. J. Vis. Exp. **42**:2038.
43. **Morris JD, Hewitt JL, Wolfe LG, Kamatkar NG, Chapman SM, Diener JM, Courtney AJ, Leevy WM, Shrout JD.** 2011. Imaging and analysis of *Pseudomonas aeruginosa* swarming and rhamnolipid production. Appl. Environ. Microbiol. **77:**8310-8317.
44. **Kaiser D, Warrick H.** 2011. *Myxococcus xanthus* swarms are driven by growth and regulated by a pacemaker. J. Bacteriol. **193:**5898-5904.
45. **Reichenbach H, Heunert HH, Kuczka H.** 1965. Myxococcus spp. (Myxobacterales)-Schwarmentwicklung und Bildung von Protocysten. Institut fur den Wissenschaftlichen Film, Gottingen, Federal Republic of Germany.
46. **Mignot T, Shaevitz JW, Hartzell PL, Zusman DR.** 2007. Evidence that focal adhesion complexes power bacterial gliding motility. Science **315:**853-856.
47. **Mignot T, Merlie JP, Jr., Zusman DR.** 2005. Regulated pole-to-pole oscillations of a bacterial gliding motility protein. Science **310:**855-857.
48. **Kimchi A, Rosenberg E.** 1976. Linkages between deoxyribonucleic acid synthesis and cell division in *Myxococcus xanthus*. J. Bacteriol. **128:**69-79.
49. **Rosario CJ, Singer M.** 2007. The *Myxococcus xanthus* developmental program can be delayed by inhibition of DNA replication. J. Bacteriol. **189:**8793-8800.
50. **Sun H, Yang Z, Shi W.** 1999. Effect of cellular filamentation on adventurous and social gliding motility of *Myxococcus xanthus*. Proc. Natl. Acad. Sci. USA **96:**15178-15183.

51. **Tzeng L, Ellis TN, Singer M.** 2006. DNA replication during aggregation phase is essential for *Myxococcus xanthus* development. J. Bacteriol. **188:**2774-2779.
52. **Leonardy S, Freymark G, Hebener S, Ellehauge E, Søgaard-Andersen L.** 2007. Coupling of protein localization and cell movements by a dynamically localized response regulator in *Myxococcus xanthus*. EMBO J. **26:**4433-4444.
53. **Zhang Y, Guzzo M, Ducret A, Li YZ, Mignot T.** 2012. A dynamic response regulator protein modulates G-protein-dependent polarity in the bacterium *Myxococcus xanthus*. PLoS Genet. **8:**e1002872.
54. **Bowden MG, Kaplan HB.** 1998. The *Myxococcus xanthus* lipopolysaccharide O-antigen is required for social motility and multicellular development. Mol. Microbiol. **30:**275-284.
55. **Pathak DT, Wei X, Bucuvalas A, Haft DH, Gerloff DL, Wall D.** 2012. Cell contact-dependent outer membrane exchange in myxobacteria: genetic determinants and mechanism. PLoS Genet. **8:**e1002626.
56. **Pathak DT, Wall D.** 2012. Identification of the *cglC*, *cglD*, *cglE*, and *cglF* genes and their role in cell contact-dependent gliding motility in *Myxococcus xanthus*. J. Bacteriol. **194:**1940-1949.
57. **Dworkin M, Kaiser D.** 1985. Cell interactions in myxobacterial growth and development. Science **230:**18-24.
58. **Wu Y, Jiang Y, Kaiser D, Alber M.** 2007. Social interactions in *Myxobacterial* swarming. PLoS Comput. Biol. **3:**e253.
59. **Conrad JC, Gibiansky ML, Jin F, Gordon VD, Motto DA, Mathewson MA, Stopka WG, Zelasko DC, Shrout JD, Wong GC.** 2011. Flagella and pili-mediated near-surface single-cell motility mechanisms in *P. aeruginosa*. Biophys. J. **100:**1608-1616.
60. **Harms A, Treuner-Lange A, Schumacher D, Søgaard-Andersen L.** 2013. Tracking of chromosome and replisome dynamics in *Myxococcus xanthus* reveals a novel chromosome arrangement. PLoS Genet. **9:**e1003802.
61. **Iniesta AA.** 2014. ParABS System in Chromosome Partitioning in the Bacterium *Myxococcus xanthus*. PLoS One **9:**e86897.
62. **Wall D, Kolenbrander PE, Kaiser D.** 1999. The Myxococcus xanthus *pilQ* (*sglA*) gene encodes a secretin homolog required for type IV pilus biogenesis, social motility, and development. J. Bacteriol. **181:**24-33.
63. **Kimsey HH, Kaiser D.** 1991. Targeted disruption of the *Myxococcus xanthus* orotidine 5'-monophosphate decarboxylase gene: effects on growth and fruiting-body development. J. Bacteriol. **173:**6790-6797.

583 **Table 1: Strain List**

M. xanthus Strain	Relevant characteristics	Source or reference
DK1622	A^+S^+; Wild-type strain	(62)
DZ2	A^+S^+; Wild-type strain	(8)
DK8621	A^+S^-; *ΔpilA* of DK1622	Kaiser collection-Wall Laboratory
DK7881	Hypo-reversing; *ΔfrzE* of DK1622	(63)
DW706	Hyper-reversing; *ΔfrzCD* of DK1622 (Mx4 transduction of *frzCD::*Tn5-132 Ω224)	Wall Laboratory
DK1240	A^-S^+; *ΔcglC6* of DK1622	(56)
DZ4483	Hypo-reversing; *ΔfrzF* of DZ2	(29)
DZ4482	Hyper-reversing; *ΔfrzG* of DZ2	(29)
JS1	P_{nat}-*romR*-gfp fusion in DK1622 (constructed using *pSH1208)*	This study, using approach in (24)
JS2	P_{nat}-*romR*-gfp fusion in DW706 (constructed using *pSH1208)*	This study, using approach in (24)

584

585 **Table 2: Predivison Pauses, Motility, and Growth Attributes of *Myxococcus xanthus***

Strain	Pause Duration* (min)	Single Cell Velocity (µm/min)	Group Expansion Rate** (µm/min)	Growth Doubling Time*** (hour)
DK1622	18.3 ± 0.8 (n = 101)	5.04 ±0.37 (n=19)	1.34 ±0.25	4.8 ± 0.6
DZ2	19.7 ± 0.8 (n = 90)	4.61 ±0.62 (n=15)	1.60 ±0.49	3.6 ± 0.1
Δ*pilA* (DK8621)	17.2 ± 0.8 (n = 97)	2.95 ±0.67 (n=15)	0.90 ±0.24	4.4 ± 0.4
ΔfrzE (DK7881)	26.5 ± 0.9 (n = 73)	2.01 ±0.58 (n=15)	0.85 ±0.21	4.1 ± 0.7
ΔfrzCD (DW706)	22.3 ± 1.0 (n = 55)	2.78 ±0.68 (n=30)	0****	4.1 ± 0.3
ΔfrzF (DZ4483)	17.7 ± 0.8 (n = 83)	not measured	0.63*****	not measured
ΔfrzG (DZ4482)	21.1 ± 1.0 (n = 59)	not measured	1.45*****	not measured

586 *Pause Duration is average ± one standard error. All other values are averages ± one standard
587 deviation.
588 **Group Expansion Rate calculated from n=3 for each strain.
589 *** Growth Doubling Time calculated from n=3 for each strain.
590 ****DW706 exhibits no overall expansion when hyper-reversing—all replicates showed no
591 expansion.
592 *****Measured in (44).
593
594

Figure Legends:

Figure 1. Sequence of motility pausing and cell division for one representative *M. xanthus* cell (DK8621). From the start of tracking (0 min), the cell moves in several directions and stops movement at 6.3 minutes, divides at roughly 25 minutes, and cells are clearly motile at 28.3 minutes. Scale bar is 10 μm.

Figure 2. Sequence of motility pausing and cell division for four *M. xanthus* DZ2 cells within a group. Initially (0-2.8 min), all cells that are motile. At 5.3 min, the cells colored blue, red and yellow have stopped. The green cell stops by 6.8 minutes while many other cells remain motile. From 6.8-18.0 minutes, these colored cells do not actively move but are subject to numerous interactions with surrounding active cells (black arrows)—this results in some change of position for the paused cells. At 20.5 minutes the blue cells have divided and have initiated motility. The remaining colored cells initiate motility by 32.0 minutes. Scale bar is 10 μm.

Figure 3. Duration of motility pauses at the time of cell division for *Myxococcus xanthus*. Mean value for each strain is indicated by the × and error bars show the standard error of the 95% confidence interval determined by mean comparison of all data points.

Figure 4. Initial motility direction of both progeny in reference to parent cell as percentage of division events for each individual strain. "Opposing" = cells initiate motility in opposing directions where leading cell inherits motility direction of parent cell. "Both leading" = both cells initiate motility in direction of parent cell. "Both lagging" = both cells initiate motility in opposite direction of parent cell. "Crossing" = cells initiate motility in opposing directions where lagging cell inherits motility direction of parent cell.

Figure 5. Dynamic distribution of RomR-GFP during division of a representative cell (colored red) that was initially moving left-to-right. A) Fluorescence intensity of RomR-GFP along a dividing cell (longitudinal axis) over time. The cell pauses motility at 2.5 min and progeny initiate motility at 22.5 min. After division, the leading cell (colored green) moves to the right while the lagging cell (colored blue) moves to the left. B) Transmission detection image, green fluorescent image, and merged image with delineated cell morphology at 5.75 min, C) 17.0 min, D) 23.25 min, and E) 26.5 min.

Figure 6. Multi-point accumulation of RomR-Gfp in a *M. xanthus frzCD* mutant strain (JS2). From left to right is the transmission detection image highlighting a paused pre-division cell and two other cells, the GFP-fluorescent channel showing RomR-Gfp, and the merged image with the cell delineation overlay highlighting the 3-4 RomR accumulation sites for each of these cells.

Figure 7. Model for cell division and polarity inheritance via diffusion of RomR in *M. xanthus*. A) A motile predivision cell moves left-to-right. RomR is localized to both poles but preferentially to the rear pole, while RomR freely diffuses in the cytoplasm. **B)** The predivisional cell pauses its motility. Key division proteins PomZ and FtsZ act to mark the cell division site and initiate separation. **C)** As FtsZ constricts the cell, this both limits diffusion of RomR across the entire volume and cues accumulation of RomR at these newly developing poles. RomR preferentially accumulates at the new pole of the lagging cell. **D)** Upon completion of cell division, these progeny display sufficiently differing polar traits to initiate motility in opposing

643 directions. Synthesis of new type IV pili may coincide with these actions but are not required to
644 initiate motility.
645

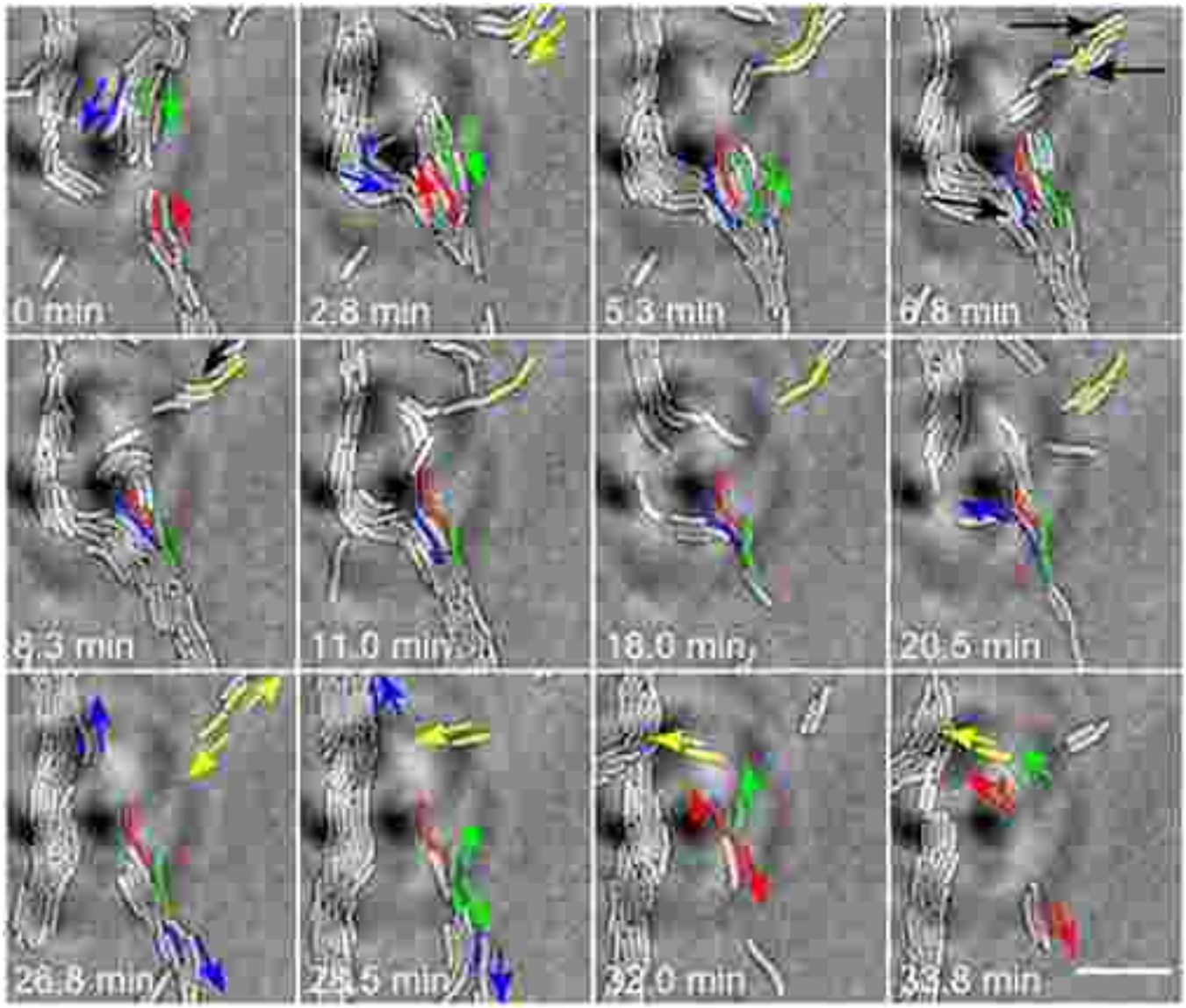

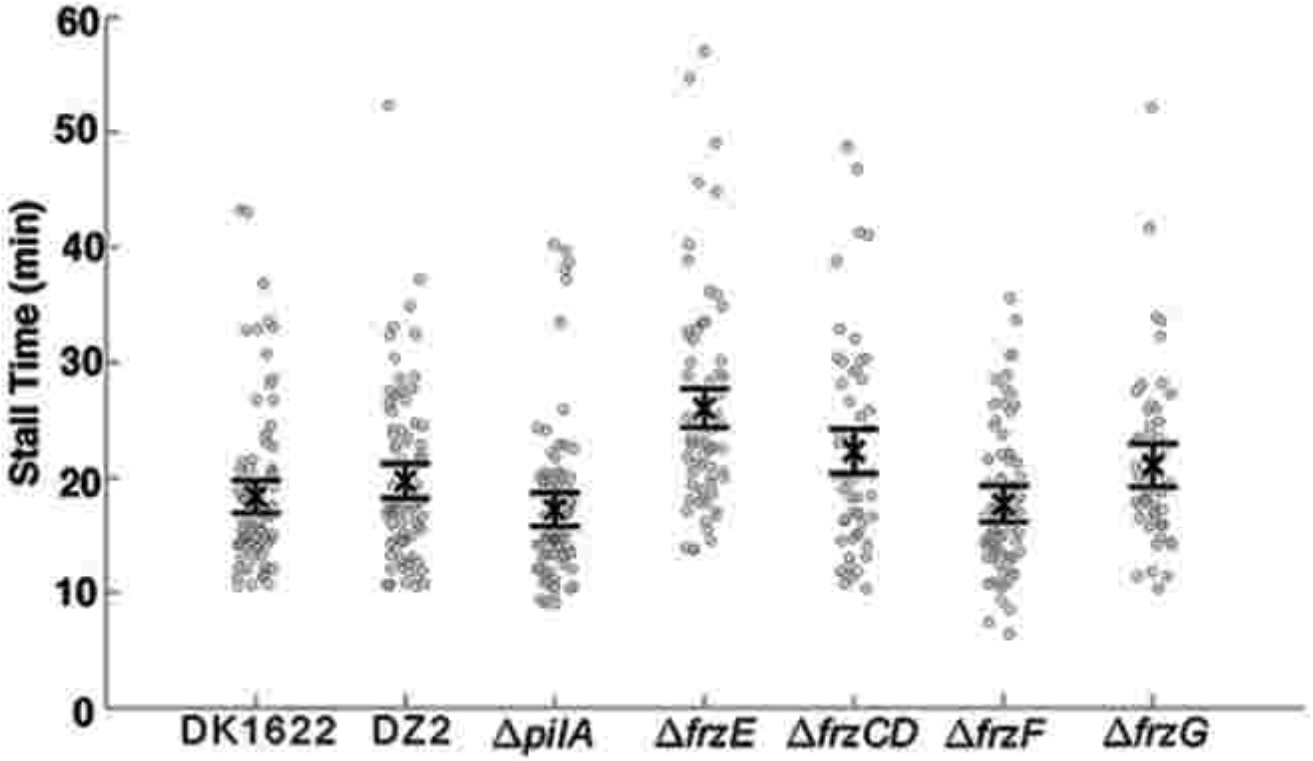

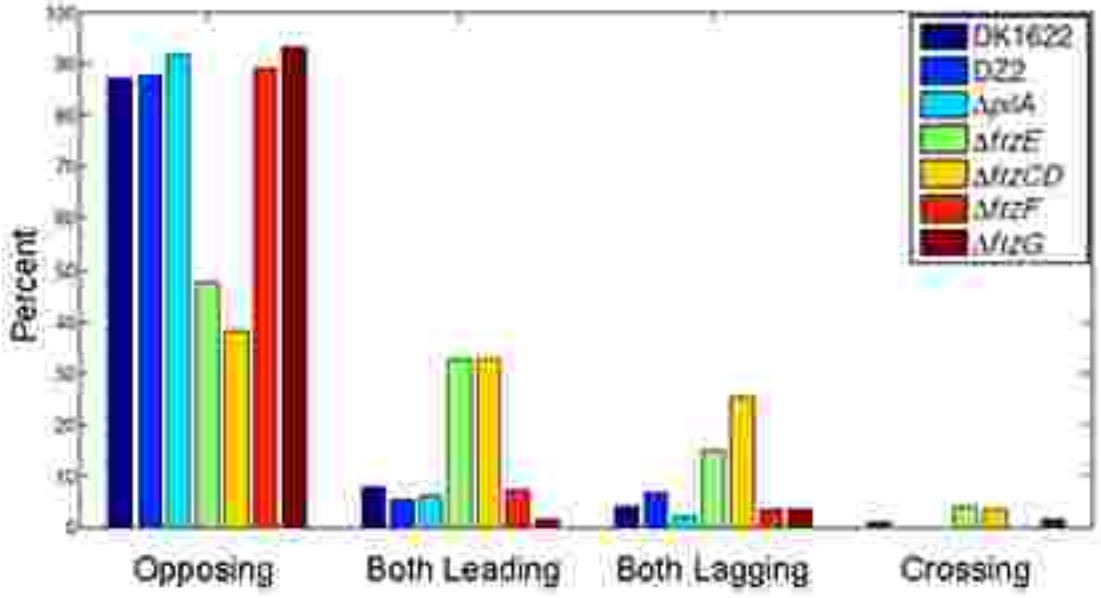

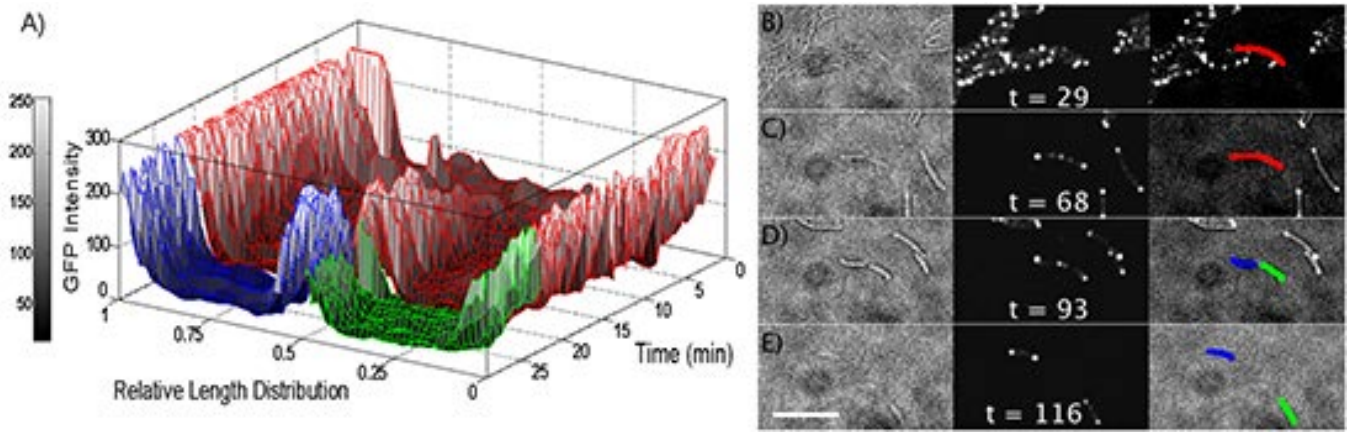

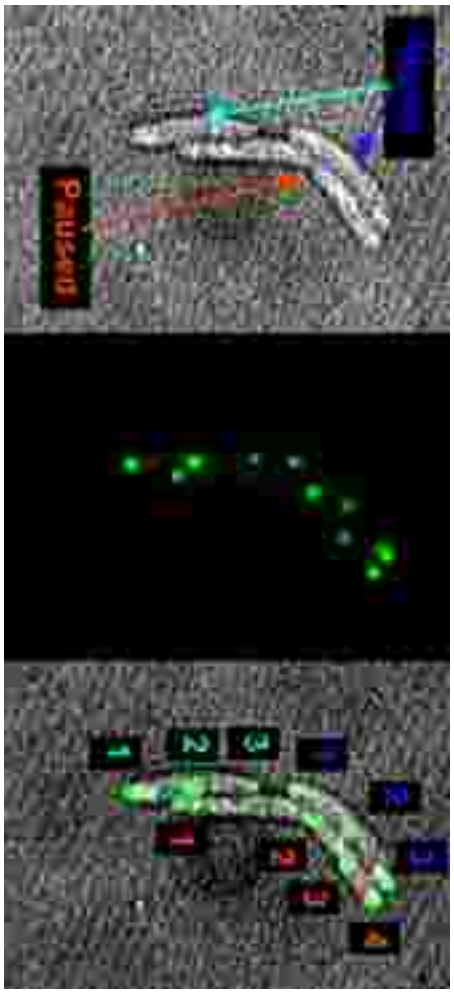
PAUSED